

## HORIZONTAL IMPEDANCE FUNCTIONS OF INCLINED SINGLE PILES

Chandra Shekhar GOIT<sup>1)</sup> and Masato SAITOH<sup>1)</sup>

<sup>1)</sup> Foundations and Earthquake Lab., Department of Civil and Environmental Engineering, Saitama University

### ABSTRACT

Horizontal impedance functions of inclined single piles are measured experimentally for model soil-pile systems with both the effects of local soil nonlinearity and resonant characteristics. Two practical pile inclinations of 5° and 10° besides a vertical pile embedded in cohesionless soil and subjected to lateral harmonic pile head loadings for a wide range of frequencies are considered. Results obtained with low-to-high amplitude of lateral loadings on model soil-pile systems encased in a laminar shear box show that the local nonlinearities have a profound impact on the horizontal impedance functions of piles. Horizontal impedance functions of inclined piles are found smaller than the vertical pile and the values decrease with the increase in the angle of pile inclination. Distinct values of horizontal impedance functions are obtained for the 'positive' and 'negative' cycles of harmonic loadings, leading to asymmetric force-displacement relationships for the inclined piles. Validation of these experimental results is carried out through three-dimensional nonlinear finite element analyses, and the results from the numerical models are in good agreement with the experimental data. Sensitivity analyses conducted on the numerical models suggest that the consideration of local nonlinearity at the vicinity of the soil-pile interface influence the response of soil-pile systems.

**KEYWORDS:** local nonlinearity, impedance functions, inclined piles, nonlinear finite element model

### 1. INTRODUCTION

A significant amount of work (Kuhlemeyer 1979, Kaynia and Kausel 1982, Dobry and Gazetas 1988, Makris and Gazetas 1992, Mylonakis et al. 1997) has been carried out in reliable prediction of the response of structures with vertical piles exposed to seismic excitations as vertical piles are undoubtedly a popular choice for a wide range of structures. Inclined piles (also referred as 'batter piles' or 'raked piles'), on the other hand, are particularly desired for structures demanding substantial lateral stiffnesses and so offshore structures, bridges, and towers are the most common examples where these piles find their applicability. However, for a considerable length of time, the use of inclined piles has been considered detrimental in seismic conditions and was restricted by design codes like AFPS 1990 and Eurocode 2000. Simple reasons for restricting the use of inclined piles include soil settlement-induced large magnitude vertical loads, excessive axial compression and pullout forces during an earthquake, and reduction in bending capacity due to seismically induced tensile forces. Field evidences such as failure of the wharf in the port of Oakland in 1989 Loma Prieta earthquake and the port of Los Angeles in 1994 Northridge earthquake are few of the examples with unsatisfactory performance of inclined piles leading to their bad

reputation.

However, recent researches on inclined piles are providing some positive aspects on their use. As reported by Gazetas and Mylonakis 1998, in recent years, evidence has been accumulating that inclined piles may, in certain case, be beneficial rather than detrimental both for the structure they support and the piles themselves. Supporting field evidence to this issue was noted in Maya Wharf during 1995 Kobe earthquake where one of the very few quay-walls that survived was a composite wall relying on inclined piles. Further to this, thorough investigation by Mitchell et al. 1991 on the failure during Loma Prieta earthquake revealed that the failure was due to improper design of reinforcements connecting piles and the pile-cap rather than the use of inclined piles itself. These encouraging facts have attracted much research interest in recent years on inclined piles. Studies by Sadek and Shahrour 2004, Okawa et al. 2005, Poulos 2006, Gerolymos et al. 2008, Kiyota et al. 2010, Padron et al. 2010, 2012 have shown that the seismic response of a structure may improve in certain aspects when supported by inclined piles.

For the structures supported by piles, it is evident that, upon the action of external force, neither the structural nor the ground displacements are independent of each other. The response of soil influences the motion of structure and the motion

of structure influences the response of soil, leading to so called ‘soil-pile-structure interaction’ (SPSI) effects. Predicting the response of structures with the consideration of such effects under dynamic loading is, however, a complex problem. One of the most widely used methods for solving such problems relies on the concept of sub-structuring, where the total response can be conveniently divided into – a) kinematic response and b) inertial response (Gazetas, 1984), as obtaining the total response of system without such sub-structuring scheme becomes quite complicated (Goit, 2008, Goit et al., 2008). For such approach, impedance functions (IFs) of piles are one of the essential components required for computing the response of pile-supported structures. For a laterally loaded pile group, three distinct associated impedance functions can be formulated pertaining to horizontal, rotational, and cross horizontal-rotational impedances. Furthermore, for footings restricted in rotation, only the horizontal component bears the practical importance. These horizontal IFs are complex-valued frequency dependent quantities and are expressed by their real and imaginary parts as

$$K_{hh}^* = k_{hh} + iC_{hh} \quad (1)$$

where  $k_{hh}$  and  $C_{hh}$  are corresponding real and imaginary parts, respectively. The real part reflects the stiffness of the soil-pile system, while the imaginary part reflects the combined action of frequency-dependent wave radiation and frequency independent material damping of the pile and soil.

Alternatively, Eq. (1) can also be presented in the following form

$$K_{hh}^* = k_{hh} + i\omega c_{hh} \quad (2)$$

where,  $c_{hh} = C_{hh} / \omega$  is the coefficient of equivalent viscous damping and  $\omega$  is the circular frequency..

It is important to note that the dynamic pile group behavior is fundamentally different from that of a single pile, and its impedance cannot be simply predicted by superimposing the impedances of its members as piles in a group are not only affected by their individual loads, but also by additional loads transferred through the soil from the neighboring piles (pile-to-pile interaction). Such pile-to-pile interactions are also frequency-dependent complex quantity.

Analytical solutions for the static stiffnesses and IFs of single vertical piles (Poulos and Davis 1980, Mylonakis and Gazetas 1999) and the static stiffnesses of single inclined piles (Poulos 1980) are available along with the numerical verifications by Giannakou et al. 2010. Also available are a number of approximate dynamic interaction-factor-

based methods (Nogami 1985, Dobry and Gazetas 1988, Makris and Gazetas 1992) in obtaining pile groups’ impedance functions. However, most of these available solutions treat soil as a linear elastic material. Applicability of this supposition of soil as a linear elastic material can be considered as a practical assumption for low-level of excitations, but under strong excitations soil near a vibrating pile behaves nonlinearly and has a strong influence on the response of piles, which cannot be captured by the elastic solutions. Only a limited number of works are available considering this nonlinear behavior of soil (Kiyota et al. 2010).

In this study, effects of local nonlinearity on the horizontal IFs of inclined single piles under strong excitations are considered. Dynamic experimental investigations on model soil-pile systems embedded in homogeneous dry sand encased in a laminated shear box were carried out under one-g conditions. A wide range of frequencies encompassing typical structural and soil periods is reported. Fixed head floating piles with pile inclinations of 5° and 10° besides a vertical pile (0°) are considered to encompass a practical range of pile inclinations. Directions of pile inclinations are along the line of the direction of loading. Experiments consider both the effects of resonance in the soil and local nonlinearities due to externally-applied loads through pile head excitations. Experimentally measured horizontal IFs are further validated using three-dimensional nonlinear finite element models.

## 2. EXPERIMENTAL METHODOLOGY

Notwithstanding that full-scale field tests may provide high quality data, such tests have well-known limitations in terms of cost, loading conditions, control mechanisms and material properties. Model tests are often essential when the prototype behavior is complex and difficult to assess. Such physical models could provide information for desired loading conditions with much flexibility in comparison to full-scale field tests. To this end, use of scaling relations relating the response of a model to that of a prototype is essential, based on similitude theory.

In the context of similitude theory, loading rate in the model is faster than in the prototype, to balance the difference in scale and stiffness between the two systems. Scaling relations for soils considering such issues were first derived by Rocha 1957 and Roscoe 1968. To relate the response of a model to that of the prototype encompassing material behavior for differing stress regimes, two scaling factors for stress and strain were proposed by Rocha. Further work was carried out by Kagawa 1978, Kokusho and Iwatate 1979, and Iai 1989 extending the theory to more general conditions.

## 2.1 Model-prototype relations

For the present experimental investigations, the scaling laws derived by Kokusho and Iwatate 1979 pertaining to one- $g$  conditions, are employed. The similitude law considers the ratio of forces acting on prototype and model, providing the law of similitude for dynamic testing of a soil by shaking table tests, suggesting the loading frequency relationship between the model and prototype as:

$$\frac{\omega_m}{\omega_p} = \eta^{-1/4} \lambda^{-3/4} \quad (3)$$

where,  $\omega_m$  is the loading frequency on the model,  $\omega_p$  is the corresponding frequency at the prototype,  $\lambda$  is the geometric scaling ratio of the model to the prototype and  $\eta$  is the density scaling ratio of the model to the prototype. In the present work, geometric scaling factor  $\lambda$  was adopted as 0.05, i.e., the model is 20 times smaller than the prototype. Furthermore, the ratio of dynamic strain between the model and prototype is given by

$$\frac{\gamma_m}{\gamma_p} = \eta^{1/2} \lambda^{1/2} \quad (4)$$

where,  $\gamma_m$  is the dynamic strain in the model and  $\gamma_p$  is the corresponding dynamic strain in the prototype. Table 1 summarizes the scaling relationship used in the present work.

## 2.2 Experimental setup

The experimental setup consists of a soil-pile system cased in a laminar shear box (1200 mm x 800 mm x 1000 mm) bolted on a digitally controlled unidirectional shaking table ( $\pm 200$  mm) owned by Saitama University as shown in Figure 1. The shear box consists of a set of rectangular metallic frames stacked on top of each other with ball bearings between each frame to minimize the

shear resistance of the housing, i.e., allowing the shear box to move freely in the horizontal shear.

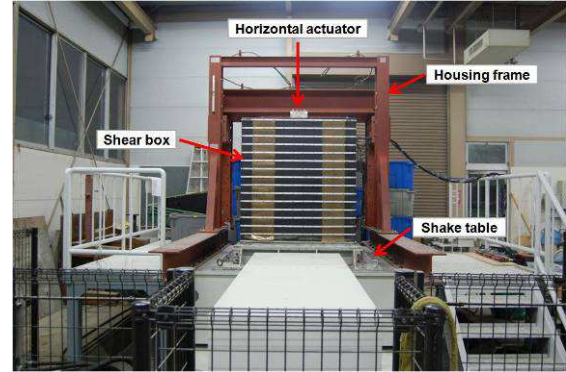


Figure 1: Details of shaking table unit

Homogeneous dry Gifu sand, found in Japan was employed. The standard properties of sand include specific gravity  $G_s = 2.643$ , coefficient of uniformity  $C_u = 1.590$ , internal angle of friction  $\phi = 27.5^\circ$  with maximum and minimum voids ratio  $e_{\max} = 1.126$  and  $e_{\min} = 0.717$ , respectively. The gradation curve showed  $D_{60} = 0.350$  mm,  $D_{30} = 0.310$  mm and  $D_{10} = 0.220$  mm with the maximum diameter of particles being 0.840 mm. To obtain the desired compaction, soil in the shear box was compacted by base vibration of shear box using the shaking table at frequency of 40 Hz and amplitude of  $5 \text{ m/s}^2$ , to a density of  $1.46 \text{ t/m}^3$  as listed in Table 1. Corresponding voids ratio was 0.81 with relative density of 77.5 %.

For piles, solid cylindrical acrylic fixed head floating piles having diameter  $d = 40$  mm and length  $L = 900$  mm were used. Solid acrylic pile head (125 mm x 125 mm x 125 mm) connected to a horizontal actuator provided the restraint for the pile head so that only horizontal translation was allowed (no rotation and vertical movements). No contact between the base of the pile head and soil was allowed to discard any resistance provided

Table 1: Model-prototype scaling relations based on Kokusho and Iwatate 1979

Items	Similitude		Scaling factors			Units
	Law	Factor	Prototype	Target	Attained	
Length of pile ( $L$ )	$\lambda$	0.05	18.0	0.90	0.90	m
Diameter of pile ( $d$ )	$\lambda$	0.05	0.80	0.04	0.04	m
Density of pile ( $\rho_p$ )	$\eta$	0.81	2.40	1.95	1.21	$\text{t/m}^3$
Young's modulus of pile ( $E_p$ )	$\eta^{1/2} \lambda^{1/2}$	0.20	25.0	5.04	3.20	GPa
Depth of soil ( $H$ )	$\lambda$	0.05	20.0	1.00	1.00	m
Density of soil ( $\rho_s$ )	$\eta$	0.81	1.80	1.46	1.46	$\text{t/m}^3$
Shear wave velocity ( $V_s$ )	$\eta^{-1/4} \lambda^{1/4}$	0.50	171.5	85.44	95.72	m/s
Natural frequency of soil ( $f_n$ )	$\eta^{-1/4} \lambda^{-3/4}$	9.96	2.14	21.36	23.93	Hz

through friction. Moreover, to prevent any possible slippage between the pile and soil, sand was adhered on the surface of the acrylic pile. Three separate cases of soil-pile systems with pile inclinations of 0°, 5° and 10° with respect to the vertical were considered. Figure 2 shows the layout of the 10° inclined pile in the shear box.

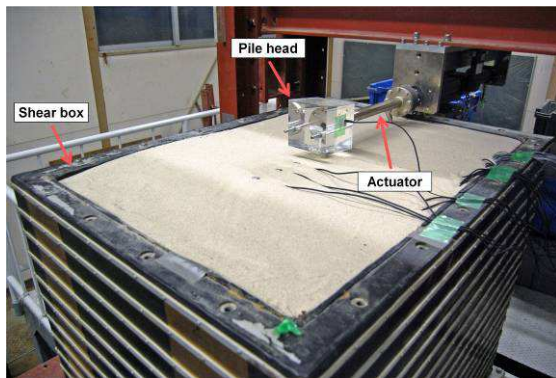
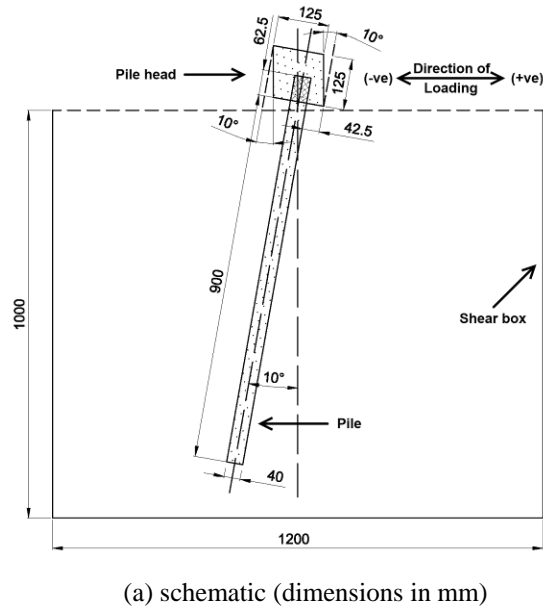


Figure 2: Inclined pile (10°) layout in shear box

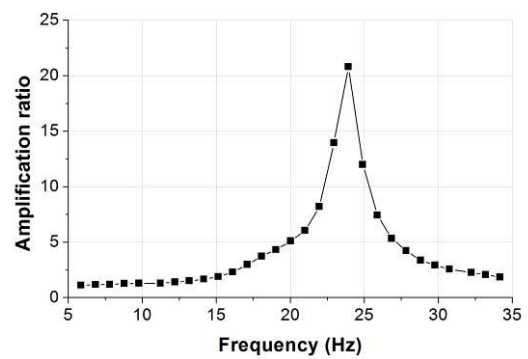
Six different amplitudes of lateral harmonic accelerations at the pile head (0.5, 1, 2, 3, 4, and 5 m/s<sup>2</sup>) were used to test the soil-pile systems in the frequency range of 6 ~ 35 Hz. A digitally controlled unidirectional hydraulic actuator ( $\pm 10$  kN,  $\pm 150$  mm) was used for the pile head loadings. To reduce the effects of noise, predominantly at higher frequencies, recorded data for the horizontal IF are passed through a narrow band-pass filter.

### 3. EXPERIMENTAL RESULTS

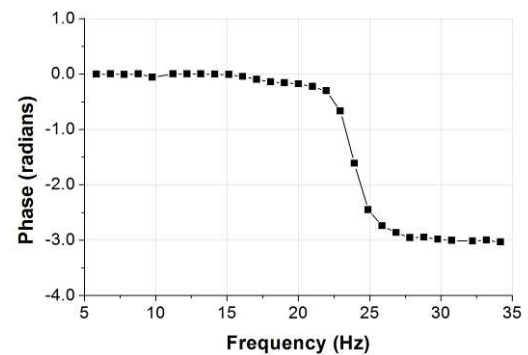
#### 3.1 Dynamic response of soil

A key first step in the present experimental framework was to obtain the elastic response of

soil for determining the equivalent elastic properties of soil mass in the absence of piles. To this end, the free field response of soil was obtained in the form of acceleration measurements with base excitation provided at the base of the shaking table. Testing was performed on a total height of 1000 mm of dry Gifu sand of relative density 77.5% with very small harmonic loading amplitude of 0.2 m/s<sup>2</sup> at the base of shear box through the shaking table. Figure 3 shows the response of this soil-only case in the frequency domain, in the form of the amplification ratio between base and soil surface, along with the phase information. The natural frequency of soil ( $f_n$ ) is approximately 24 Hz.



(a) amplification



(b) phase

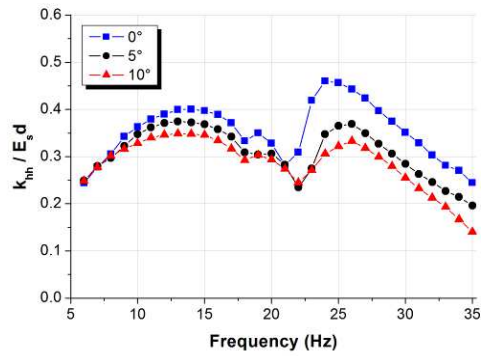
Figure 3: Elastic response of soil

The mean shear strain in soil due to the applied small amplitude loading is of the order  $1.84 \times 10^{-4}$ , which may be used as a reference case associated with essentially linear soil behavior. Corresponding low-strain Young's modulus of elasticity ( $E_s$ ) of soil is approximately 39 MPa.

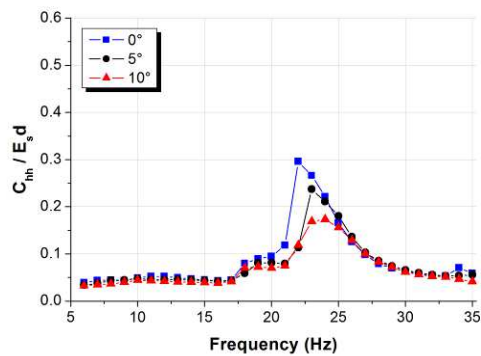
#### 3.2 Horizontal impedance functions

Applied lateral harmonic loadings in the form of accelerations at the pile head lead to two individual values of reaction forces pertaining to the 'positive' and 'negative' cycles of loading (stroke direction as denoted by '+ve' and '-ve' in

Figure 2 (a)). This in turn provides distinct values of horizontal IFs at the pile head for the corresponding cycles of loading. In the interest of space, comparative plots of the average values of horizontal IFs obtained from the ‘positive’ and ‘negative’ cycles of loading for vertical ( $0^\circ$ ) and inclined piles ( $5^\circ$  and  $10^\circ$ ) for a medium level loading amplitudes of  $2 \text{ m/s}^2$  is presented in Figure 4 in the frequency domain, as normalized unitless quantities.



(a) real part



(b) imaginary part

Figure 4: Horizontal impedance functions for acceleration amplitude of  $2 \text{ m/s}^2$

Results show that the horizontal IFs of single piles decrease with the increase in the angle of pile inclination for increasing frequency of loading (similar results are obtained for all other loading amplitudes). This is in contrast to the general understanding that inclined piles possess higher dynamic stiffnesses than vertical piles. The latter statement is particularly true when considering both the soil and pile as linear elastic materials, the details of which are discussed in the latter part of this paper.

Effects of pile inclinations on the horizontal IFs of piles are minimal at very low frequencies of loading (i.e., less than 10 Hz). At these frequencies, the IFs of inclined piles are approximately identical to the vertical pile at all loading amplitudes. Resonance of soil-pile systems is distinctly observed for all amplitude of loadings within the

measured range of frequency. For  $2 \text{ m/s}^2$  amplitude of loading, the resonant frequency of soil-pile systems is around 23 Hz. Additionally, reflection of resonant frequency is clearly seen on the imaginary part of the plots in terms of the increase in damping triggered by wave propagation in soil.

For the frequencies greater than 10 Hz, the vertical pile shows the highest value of IFs followed by inclined pile with the inclination of  $5^\circ$ , while the pile with  $10^\circ$  inclination shows the lowest value. The difference between the individual IFs of piles, however, becomes narrower with the increase in the loading amplitude. As for the imaginary part of IFs, the vertical pile shows the highest value predominantly at the resonant frequency of the soil-pile systems. Moreover, the peak values for all pile inclinations saturate to almost a constant value equal to that of the vertical pile at the resonant frequency for higher loading amplitudes.

### 3.3 Force-displacement relationships

Differences between IFs corresponding to the ‘positive’ and ‘negative’ cycles of loading for the vertical and inclined piles are better identified through force-displacement relationships. For this purpose, a sample loading frequency of 25 Hz is considered. Experimentally recorded data are passed through a low-pass filter with cut-off frequency of 1.5 times the frequency under consideration to remove any existing high-frequency components from the data and to have a clear distinction in the response between the ‘positive’ and ‘negative’ cycles of loading. Figure 5 shows the comparative force-displacement relationship between the vertical and inclined piles.

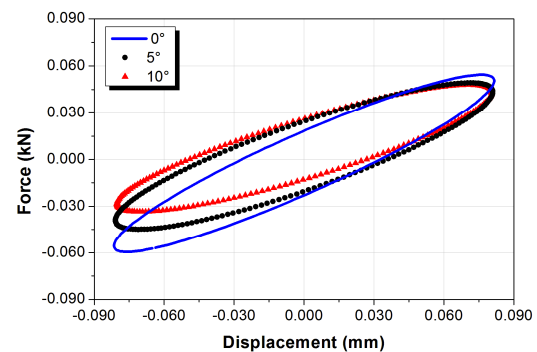


Figure 5: Experimental force-displacement curves for loading amplitude of  $2 \text{ m/s}^2$  at 25 Hz

Figure 5 shows that the peak reaction forces in the ‘positive’ loading direction approximately maintain an identical value for both the vertical and inclined piles, but in the ‘negative’ loading direction, peak reaction forces for inclined piles decrease almost in linear proportion with the increase in the angle of pile inclination. This observed asymmetric responses of inclined piles corresponding to the ‘positive’ and ‘negative’

cycles of loading can be attributed to the local nonlinearities at the vicinity of the soil-pile interface, the evidence of which was observed during experiments and is shown in Figure 6. Vertical pile, on the other hand, shows almost perfect symmetric force-displacement curves for the entire frequency range.

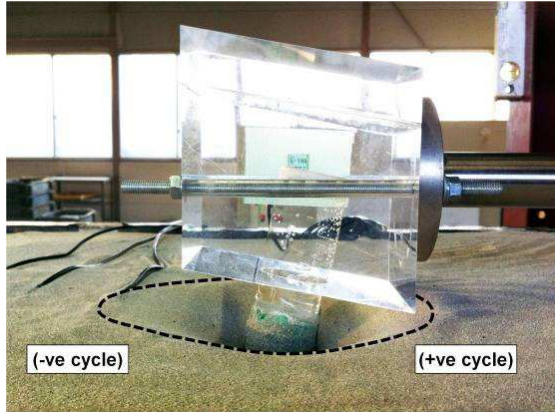


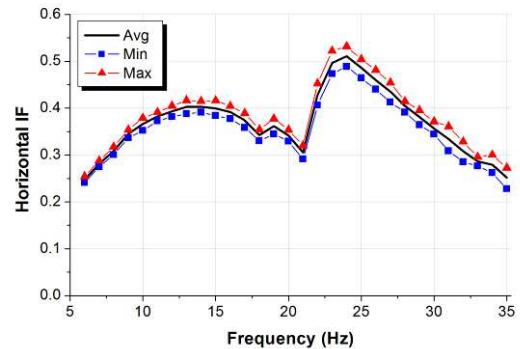
Figure 6: Experimental asymmetric behavior for 10° inclined pile

Figure 7 shows the plots of maximum, minimum and average values of horizontal IFs based on force-displacement curves corresponding to the ‘positive’ and ‘negative’ cycles of loading for the recorded frequency range. Plots are presented in the form of normalized magnitudes of IFs, with an identical normalizing factor as for Figure 4. Only 0° and 10° piles corresponding to the vertical and maximum pile inclination in the present work are reported. Due to near-perfect symmetric force-displacement curves for the vertical pile, the difference between the maximum and minimum values of IFs is almost negligible as seen from Figure 7 (a). For the inclined pile, on the other hand, there is a considerable difference between the maximum and minimum values as seen from Figure 7 (b).

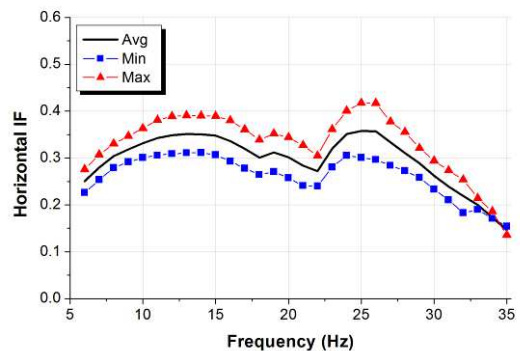
Experimental observations and obtained results (validated by numerical analyses and detailed in subsequent section) suggest the existence of separation between the pile and soil for the entire range of recorded frequency. The piles undergoing lateral deflections inevitably mobilize passive-type soil failure in front of the piles accompanied by gap formation and sliding in the rear and the sides of the piles, respectively. Such gaps created due to the tensile failure in the rear of the piles, in principle, are almost immediately filled by the collapse of surrounding soil due to its cohesionless characteristics.

For the ‘negative’ cycle of loading, the gap formed in the rear of the vertical pile is easily filled by the collapse of surrounding soil, maintaining contact with the pile on both sides. However, with a relative stable geometric configuration of soil in

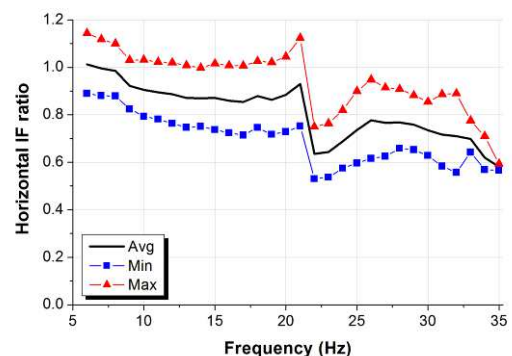
the rear for the inclined pile, the entire depth of the gap between the pile and soil cannot be filled by the collapsed soil, and the gap remains. This leads to a lesser depth of soil contact for the inclined pile suggesting that the pile has effective support on only one side over most of the deformation and thus results into smaller reaction forces than the vertical pile. This is reflected in Figure 7 (c) showing that the minimum values of IFs for the inclined pile are smaller than the vertical pile for the entire frequency range.



(a) vertical pile (0°)



(b) inclined pile (10°)



(c) ratio of 10° / 0°

Figure 7: Maximum, minimum and average horizontal impedance functions for 2 m/s<sup>2</sup>

For the ‘positive’ cycle of loading, in contrast, the gap created in the rear of the inclined pile is easily filled by the collapse of surrounding soil due

to its ease of mobilization owing to the geometric layout. This suggests that the greater length of contact with soil is maintained in the rear of the inclined pile than the vertical pile, but is highly frequency dependent. Very low frequencies of loading (i.e., less than 10 Hz) results in a wider gap formation between the pile and soil due to higher applied displacements at the pile head. Such wider gaps are easily filled by the collapsed surrounding soil and thus the pile maintains contact with the soil on both sides. With the contact on both sides of the pile, the inclined pile shows higher reaction force than the vertical pile, and the reflection of this are seen in Figure 7 (c). It is interesting to note that the obtained results at these frequencies are, in fact, comparable with available elastic solutions by Poulos and Davis 1980 and subsequent findings by Giannakou et al. 2010 and Padron et al. 2010 for homogenous soil at static conditions, though the local nonlinearity at the vicinity of the soil-pile interface is accounted in the experimental models. This can be attributed to the fact that the contact conditions achieved at these very low frequencies for the inclined pile are approximately similar to that of the elastic solutions (i.e., perfect contact on both sides of piles).

As the applied displacements decrease with the increase in the loading frequency, the widths of the gap decrease. Such widths eventually become close to or less than the particle size of sand itself and can no longer be filled by the collapsed surrounding soil, leading to a greater depth of separation. Figure 7 (c) suggests that for the high-frequency region, the inclined pile shows relatively narrower width and in turn greater depth of the gap than the vertical pile, thus showing smaller values of IFs, validation of which are carried out through numerical analyses and are detailed in the following section.

#### 4. NUMERICAL MODELING

Validation of experimental results with asymmetric nature of force-displacement curves for inclined piles and therefore smaller values of IFs is carried out through three-dimensional nonlinear finite element modeling. Harmonic loading amplitude of  $2 \text{ m/s}^2$  at the pile head has been selected as the representative loading case with loading frequency of 25 Hz to serve as a companion to Figure 5. Furthermore, only  $0^\circ$  and  $10^\circ$  piles corresponding to the vertical and maximum pile inclination are considered.

##### 4.1 Model properties

Both the soil and pile are modeled as eight-noded solid elements. Length and width of the models are considered larger in comparison to the tested experimental models to remove boundary effects on the response of piles, if any. To reduce the computational time through benefit of

symmetry, only half the model is analyzed. Numerical analyses are carried out using nonlinear finite element software – Marc.Mentat v2010. A total of 13644 elements are used for soil while 38 elements are used to model the pile. As a valid practical approximation, equivalent rectangular pile sections are modeled. Figure 8 shows the finite element meshes for vertical ( $0^\circ$ ) and inclined ( $10^\circ$ ) piles.

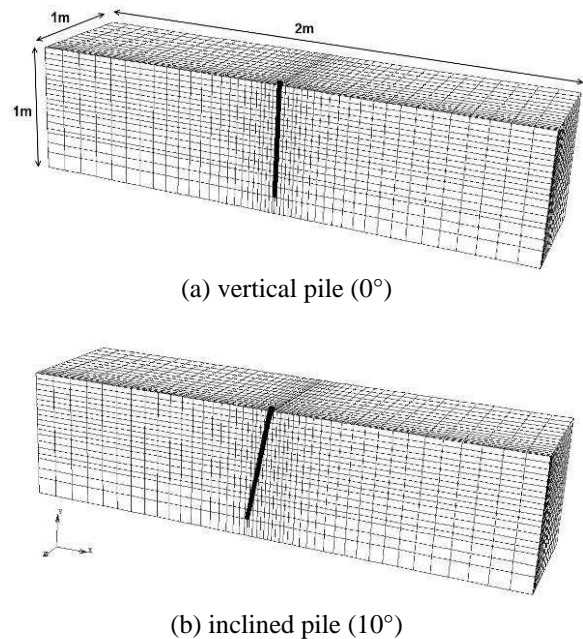


Figure 8: 3D FEM models for vertical and inclined piles

The nonlinear behavior of soil is modeled using linear Mohr-Coulomb failure criteria (elastic perfectly plastic) while the pile is modeled as a linear elastic material. Constraints are imposed on the edges of the models allowing it to move in horizontal shear as a free field. Viscous dampers are employed at the edges (so called ‘transmitting boundaries’) in all three directions for absorbing wave energy emitted from the oscillating pile, notably in the high-frequency region. Head of the pile is fixed in all directions, but the horizontal to simulate experimental conditions. Friction coefficient corresponding to the internal angle of friction of Gifu sand is considered for the pile-soil interface to simulate pile-soil interface nonlinearity, allowing soil and pile to separate under higher amplitude of loading. Initial Young’s modulus of elasticity for the models is the same as the Young’s modulus of elasticity of soil ( $E_s$ ) measured experimentally under low-strain conditions. Besides, both the geometric and material properties for the numerical models confirm to the experimental model. Stepping procedure relies on a constant time step approach with a time step of 0.001 seconds. Full Newton-Raphson method is considered for the iterative procedures.

#### 4.2 Force-displacement relationships

Figure 9 shows the comparison of force-displacement curves between the vertical and inclined piles. As for the experimental data, results from numerical analyses are also passed through a low-pass filter with cut-off frequency of 1.5 times the frequency under consideration. In line with the experimental results, results from the 3D nonlinear finite element analyses show distinct values of minimum reaction force for vertical and inclined piles under the ‘negative’ cycle of loading.

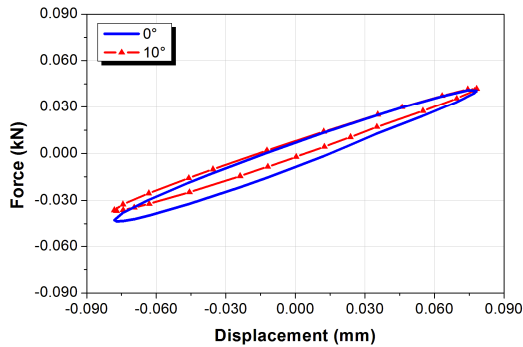


Figure 9: Numerical force-displacement curves for loading amplitude of  $2 \text{ m/s}^2$  at 25 Hz

#### 4.3 Comparison with experimental results

Based on the force-displacement relationships presented in Figure 9, ratios of maximum, minimum and average values of IFs between the inclined pile and the vertical pile are computed ( $10^\circ / 0^\circ$ ). Such obtained values are compared with the corresponding experimental results presented in Figure 7 (c). Figure 10 shows the comparison between the experimental and numerical results for the average value of IFs. The plot suggests a satisfactory agreement between the results for the experimental and three-dimensional nonlinear numerical models, ascertaining that the IFs of inclined piles are smaller than the vertical pile under nonlinear conditions.

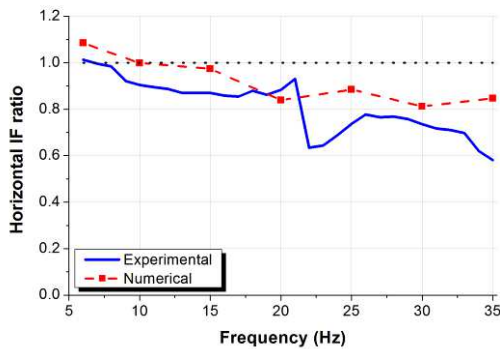


Figure 10: Comparison of experimental and numerical horizontal impedance functions ratio ( $10^\circ / 0^\circ$ )

#### 4.4 Effects of interface nonlinearity

Sensitivity of the models is tested for the pile-soil interface nonlinearity conditions. Besides modeling the separable behavior of soil-pile interfaces, additional case comprising of glued interfaces is considered (i.e., no allowance for gap formation between the soil and pile). Figure 11 shows the comparison between such cases.

For glued interfaces, both the vertical and inclined piles show near symmetric force-displacement relationships with the value of reaction forces being up to three times higher than for the case of separable interfaces, though the nonlinear behavior of soil is considered in the models. Results from this analysis for pile-soil interface nonlinearity clearly show that the consideration of perfect bonding between the pile and soil overestimates the reaction force and in turn the IFs of piles. This implies that the consideration of pile-soil interface nonlinearity largely affects the response of piles.

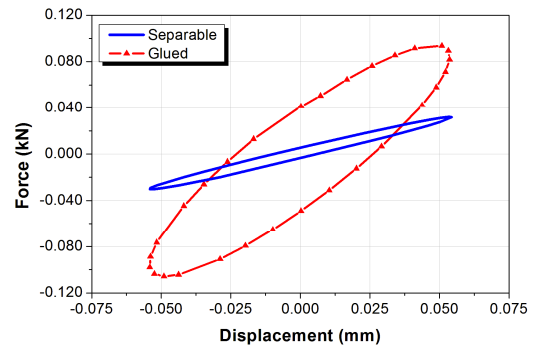


Figure 11: Effect of pile-soil interface nonlinearity on force-displacement relationships ( $10^\circ$ )

#### 4.5 Linear analysis

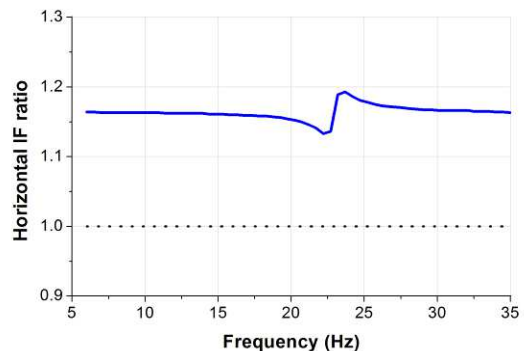


Figure 12: Horizontal impedance function ratio ( $10^\circ / 0^\circ$ ) for linear analysis

Sensitivity of the present finite element models is also tested for the material behavior of soil. In addition to nonlinear analyses to validate the experimental results, a separate case

considering soil as a linear elastic material is considered. No separation between the pile and soil is allowed, i.e., perfect bonding conditions are maintained. Results from this linear harmonic analysis case for the ratio of IFs between the inclined pile and the vertical pile ( $10^\circ / 0^\circ$ ) are presented in Figure 12. Resonance of soil-pile systems shows slight deviation in otherwise uniform mean value of this ratio for all frequencies. Obtained results show that the IFs of the inclined pile is always higher than the vertical pile for the entire frequency range considered and confirm with the published results (Padron et al. 2010). In addition, these results also agree with the experimentally obtained results for the maximum horizontal IFs at very low frequencies as presented in Figure 7(c).

## 5. CONCLUSIONS

Present experimental investigations show profound influence of local nonlinearity at the vicinity of the soil-pile interface on the horizontal impedance functions of single piles. Horizontal impedance functions of inclined single piles are found smaller than the vertical pile and the values decrease with the increase in the angle of pile inclination. Validation of the experimental results is carried out through three-dimensional nonlinear finite element analyses, and the obtained results from the numerical models are in good agreement with the experimental models. The results reveal that the asymmetric response of inclined piles leads to smaller values of horizontal impedance functions in comparison to the vertical pile.

Results obtained from the linear harmonic analyses of the numerical models for present work are found to overestimate the horizontal impedance functions of inclined single piles in comparison to the nonlinear analyses. Furthermore, sensitivity analyses conducted on the numerical models emphasize the significance of pile-soil interface nonlinearity. Through present investigations, it is shown that the consideration of local nonlinearity of soil along with the pile-soil interface nonlinearity affects the response of soil-pile systems.

Noting that a distinct maximum and minimum values of horizontal impedance functions exist depending on the direction of loading for the inclined piles, due considerations are required for designing inclined single piles to eliminate any non-conservative design. Nonetheless, it has to be noted that the present work is limited to cohesionless soils and for a single general configuration only. Furthermore, the observed behavior of pile-soil separation, in reality, occurs in soils having appreciable self-standing height. Therefore, inclined single piles surrounded by unsaturated sand could be one of the possible practical conditions where such obtained findings

can appropriately be applied. Further work is essential in understanding the behavior of inclined single piles for different soil types and conditions.

## 6. REFERENCES

AFPS, Association Francaise de Genie Paraismique (1990) “*Recommendations AFPS 90*”, Presses des Ponts et Chaussees, France.

Dobry, R. and Gazetas, G. (1988) “Simple method for dynamic stiffness and damping of floating pile groups”, *Géotechnique*, **V. 38**, (No. 4), pp. 557-574.

Eurocode (2000) “Structures in seismic regions, Part 5: Foundations, retaining structures and geotechnical aspects”, *Seismic Eurocode EC8*, European Committee for Standardization, Belgium.

Gazetas, G. and Mylonakis, G. (1998) “Seismic soil-structure interaction: new evidence and emerging issues”, *Geotechnical Earthquake Engineering and Soil Dynamics III*, ASCE, Geotechnical Special Publication, **V. 2**, pp. 1119-1174.

Gerolymos, N., Giannakou, A., Anastasopoulos, I. and Gazetas, G. (2008) “Evidence of beneficial role of inclined piles: observations and summary of numerical analyses”, *Bulletin of Earthquake Engineering*, **V. 6**, (No. 4), pp. 705-722.

Giannakou, A., Gerolymos, N., Gazetas, G., Tazoh, T. and Anastasopoulos, I. (2010) “Seismic behavior of batter piles: elastic response”, *Journal of Geotechnical and Geoenvironmental Engineering*, ASCE, **V. 139**, (No. 9), pp. 1187-1199.

Goit, C. S. (2008) “Dynamic response of piles influenced by strong ground motion”, *Master's thesis*, Saitama University.

Goit, C. S., Saitoh, M., Kawakami, H. and Nishiyama, S. (2008) “Experimental Studies on Non-Linear Response of Soil-Pile-Structure Systems Subjected to Strong Ground Motion”, *14<sup>th</sup> World Conference on Earthquake Engineering*, Beijing, October 12-17.

Iai, S. (1989) “Similitude for shaking table tests on soil-structure-fluid model in 1g gravitational field”, *Japanese Society of Soil Mechanics and Foundation Engineering*, Soils and Foundations, **V. 29**, (No. 1), pp. 105-119.

Kagawa, T. (1978) “On the Similitude in Model Vibration Tests of Earth-Structures”, *Proceedings of Japan Society of Civil Engineers*,

V. 275, pp. 69-77. [in Japanese].

Kaynia, A. M. and Kausel, E. (1982) "Dynamic stiffness and seismic response of pile groups", *Research Report*, R82-03, Massachusetts Institute of Technology.

Kiyota S., Yonezawa, T., Aoki, H., Koda, M., Nishioka, H. and Dewa, T. (2010) "Study on lateral resistance and application to railway structures of batter pile foundation", *Japan Geotechnical Journal*, V. 2, pp. 293-307. [in Japanese].

Kokusho, T. and Iwatate, T. (1979) "Scaled model tests and numerical analyses on nonlinear dynamic response of soft grounds", *Proceedings of Japanese Society of Civil Engineers*, V. 285, pp. 57-67. [in Japanese].

Kuhlemeyer, R. L. (1979) "Static and dynamic laterally loaded piles", *Journal of Geotechnical Engineering*, ASCE, V. 105, pp. 289-304.

Makris, N. and Gazetas, G. (1992) "Dynamic pile-soil-pile interaction. Part II: Lateral and seismic response", *Earthquake Engineering and Structural Dynamics*, V. 21, pp. 145 – 162.

Mitchell, D., Tinawi, R., and Sexsmith, R.G. (1991) "Performance of bridges in the 1989 Loma Prieta earthquake - lessons for Canadian designers", *Canadian Journal of Civil Engineering*, V. 18, (No. 4), pp. 711-734.

Mylonakis, G., Nikolaou, A. and Gazetas G. (1997) "Soil-Pile-Bridge Seismic Interaction: Kinematic and Inertial Effects. Part I: Soft Soil", *Earthquake Engineering and Structural Dynamics*, V. 26, pp. 337-359.

Mylonakis, G. and Gazetas, G. (1999) "Lateral vibration and internal forces of grouped piles in layered soil", *Journal of Geotechnical and Geoenvironmental Engineering*, ASCE, V. 125, (No. 1), pp. 16-25.

Okawa, K., Kamei, H., Zhang, F. and Kimura, M. (2005) "Seismic performance of group-pile foundation with inclined piles", *Proceedings of 1<sup>st</sup> Greece-Japan Workshop*, Athens, October 11-12.

Padron, L. A., Aznarez, J. J., Maeso, O. and Santana, A. (2010) "Dynamic stiffness of deep foundations with inclined piles", *Earthquake Engineering and Structural Dynamics*, V. 39, pp. 1343-1367.

Padron, L. A., Aznarez, J. J., Maeso, O. and

Saitoh, M. (2012) "Impedance functions of end-bearing piles", *Soil Dynamics and Earthquake Engineering*, V. 38, pp. 97-108.

Poulos, H. G. and Davis, E. H. (1980) "*Pile foundation analysis and design*", John Wiley & Sons, New York.

Poulos, H. G. (1980) "An approach for the analysis of offshore pile groups", *Numerical methods in offshore piling*, Institution of Civil Engineers, London, pp. 119-126.

Poulos, H. G. (2006) "Raked piles – virtues and drawbacks", *Journal of Geotechnical and Geoenvironmental Engineering*, ASCE, V. 132, (No. 6), pp. 795-803.

Rocha, M. (1957) "The possibility of solving soil mechanics problems by the use of models", *Proceedings of 4<sup>th</sup> International Conference on Soil Mechanics*, London, pp. 183-188.

Roscoe, K. H. (1968) "Soils and model tests", *Proceedings of Institute of Mechanical Engineers*, The Journal of Strain Analysis for Engineering Design, V. 3, (No. 1), pp. 57-64.

Sadek M. and Shahrour, I. (2004) "Three-dimensional finite element analysis of the seismic behavior of inclined micropiles", *Soil Dynamics and Earthquake Engineering*, V. 24, pp. 473-485.

## 7. ACKNOWLEDGEMENTS

This work was supported by Maeda Engineering Foundation, Japan. Any opinions, findings, conclusions, or recommendations expressed in this material are those of the authors and do not necessarily reflect the views of the sponsors.

The final publication of this work is available at <http://link.springer.com/article/10.1007/s11803-013-0158-0>.